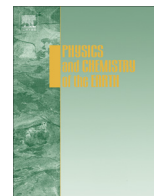




Contents lists available at ScienceDirect

Physics and Chemistry of the Earth

journal homepage: www.elsevier.com/locate/pceDocking ^{90}Sr radionuclide in cement: An atomistic modeling studyMostafa Youssef^a, Roland J.-M. Pellenq^{b,c,*}, Bilge Yildiz^{a,*}^a Laboratory for Electrochemical Interfaces, Department of Nuclear Science and Engineering, Massachusetts Institute of Technology, 77 Massachusetts Avenue, Cambridge, MA 02139, USA^b Department of Civil and Environmental Engineering, Massachusetts Institute of Technology, 77 Massachusetts Avenue, Cambridge, MA 02139, USA^c <MSE>², the CNRS-MIT Joint Laboratory, Massachusetts Institute of Technology, 77 Massachusetts Avenue, Cambridge, MA 02139, USA

ARTICLE INFO

Article history:

Available online xxx

Keywords:

Molecular simulation
Cement
Nuclear waste storage
Mechanical properties

ABSTRACT

Cementitious materials are considered to be a waste form for the ultimate disposal of radioactive materials in geological repositories. We investigated by means of atomistic simulations the encapsulation of strontium-90, an important radionuclide, in calcium-silicate-hydrate (C-S-H) and its crystalline analog, the 9 Å-tobermorite. C-S-H is the major binding phase of cement. Strontium was shown to energetically favor substituting calcium in the interlayer sites in C-S-H and 9 Å-tobermorite with the trend more pronounced in the latter. The integrity of the silicate chains in both cementitious waste forms were not affected by strontium substitution within the time span of molecular dynamics simulation. Finally, we observed a limited degradation of the mechanical properties in the strontium-containing cementitious waste form with the increasing strontium concentration. These results suggest the cement hydrate as a good candidate for immobilizing radioactive strontium.

© 2013 Elsevier Ltd. All rights reserved.

1. Introduction

The management and disposal of radioactive waste produced by the industry, medicine, radioisotope production facilities, fuel processing plants and the spent nuclear fuel are major challenges. In most countries the preferred technological approach is the disposal of the radioactive waste in repositories constructed in rock formations hundreds of meters below the earth surface (Ansolabehere et al., 2003).

Cementitious materials can be used for different purposes in the near field of the radioactive waste repository. For example, they can be used as a shielded cask to protect the waste package, as grouting for sealing cracks in the repository, as liners for the repository tunnels or most importantly as the inner most waste form itself (Evans, 2008; Komarneni et al., 1988; Wieland et al., 2006). As a waste form, the cement matrix is capable of immobilizing radionuclides. However, the mechanism of immobilization is very species sensitive (Evans, 2008) which implies that an effort has to be devoted to understand the interaction of each radionuclide with the cement matrix.

Understanding on a fundamental level the long-term performance of cement-based materials as waste forms and developing capabilities to project their lifetimes is of utmost importance. To

that end we believe that atomistic simulation is able to provide such a fundamental understanding and can be utilized as a predictive tool as well. Historically atomistic simulation was not used in cement science because of the absence of a realistic model to represent the major binding phase of cement, the poorly-crystallized calcium-silicate-hydrate (C-S-H). However, with the recent advances in our understanding of the structure of C-S-H at the nanoscale (Allen et al., 2007; Kalinichev et al., 2007; Pellenq et al., 2009), it is possible to incorporate atomistic simulation techniques in studying cementitious materials on equal footing with experiments.

C-S-H is the cementitious phase responsible for the uptake of radioactive metal cations (Wieland et al., 2006). Moreover, cation exchange is regarded as one of the key processes that regulate the uptake of metal cations in C-S-H (Mandaliev et al., 2010a; Tits et al., 2006). The immobilization by cation exchange is not limited to the disordered C-S-H in the actual cement paste, but it can also take place in a crystalline family of C-S-H named tobermorite (Komarneni and Roy, 1983; Komarneni et al., 1988; Mandaliev et al., 2010b). In this study we consider the cationic exchange as a mechanism for radioactive metal cations immobilization in both the disordered C-S-H and a member of the tobermorite family which is 9 Å-tobermorite.

The spent nuclear fuel is the most challenging source of radioactivity. At different times, different radionuclides are the dominant contributors to the overall radioactivity, radiotoxicity and decay heat emitted by the spent fuel. The two fission products strontium-90 and cesium-137 account for the bulk radioactivity

* Corresponding authors. Address: Department of Civil and Environmental Engineering, Massachusetts Institute of Technology, 77 Massachusetts Avenue, Cambridge, MA 02139, USA. Tel.: +1 617 253 7117 (R. Pellenq), +1 617 324 4009 (B. Yildiz).

E-mail addresses: pellenq@mit.edu (R.J.-M. Pellenq), byildiz@mit.edu (B. Yildiz).

for the next several decades right after the fuel discharge. Thereafter, the actinides become the dominant contributors to the radioactivity (Ansolabehere et al., 2003). Thus, it is more urgent at this stage to understand the immobilization mechanism of $^{90}\text{Sr}^{2+}$ and $^{137}\text{Cs}^+$ and to evaluate the structural and mechanical integrity of the waste form that encapsulates these radionuclides.

In this work, we focus on encapsulating $^{90}\text{Sr}^{2+}$ in the disordered C–S–H and 9 Å-tobermorite. It is known that the cation exchange $\text{Sr}^{2+} \leftrightarrow \text{Ca}^{2+}$ is the mechanism of immobilizing $^{90}\text{Sr}^{2+}$ in C–S–H (Evans, 2008; Tits et al., 2006; Wieland et al., 2008) and tobermorite (Komarneni et al., 1986; Ma et al., 1996). In fact it was shown that tobermorite exhibits partial to complete exchange of Ca^{2+} for divalent cations (Komarneni et al., 1986). However, the exchange sites, and the effect on the stability and mechanical integrity of the waste form are uncertain.

Using a combination of static structure optimization and molecular dynamics we showed that cationic exchange $\text{Sr}^{2+} \leftrightarrow \text{Ca}^{2+}$ is most likely to take place in the interlayer space of both C–S–H and 9 Å-tobermorite. Moreover this exchange does not affect the structural integrity of the silicate chains of any of the cementitious waste forms. However, this cationic exchange has an overall degrading impact on the mechanical properties of C–S–H. The organization of this paper is as follows: In the next section we describe computational approach including the force field, the simulation setup and the structural models of the C–S–H and 9 Å-tobermorite. Subsequently, we present and discuss our findings, and finally conclude with remarks about future work.

2. Computational approach

2.1. Force fields

In this work we adopted a force field that is based on representing anions polarization by the shell model of Dick and Overhauser (1958). Hereafter this force field will be referred to by *core-shell*. The core-shell force field uses the formal charges for all ions (except water oxygen and hydrogen) and this guarantees charge neutrality of any system under consideration. The parameters of this transferable force field have been optimized by many researchers to study bulk oxides (Lewis and Catlow, 1985) minerals surfaces (Kundu et al., 2005) and minerals/aqueous solutions interface (Kerisit et al., 2005, 2006; Spagnoli et al., 2006). The water component of this force field was originally introduced by de Leeuw and Parker (1998) and a major revision for the hydrogen bond representation has been introduced by Kerisit and Parker (2004).

The strontium–water potential was derived by Kerisit and Parker (2004) while strontium–layer oxygen potential is based on the work of Lewis and Catlow (1985). The strontium–layer oxygen potential was successfully used in modeling cationic exchange in zeolites (Higgins et al., 2002). Finally, we derived the strontium–hydroxyl potential from the strontium–layer oxygen potential by standard mixing rules by fixing the Buckingham (ρ) parameter and scaling the (A) parameter. All interaction potential parameters are given in the Appendix. Columbic interactions were computed using the Ewald summation method (Allen and Tildesley, 1987) with a precision of 1.0×10^{-8} .

2.2. Static structure optimization and molecular dynamics

The main purpose of static structure optimization is achieving a reasonable structure that is consequently used in the finite temperature molecular dynamics simulations. We used the code General Utility Lattice Program (GULP) (Gale, 1996; Gale and Rohl, 2003) to perform the optimization at zero pressure. Second-order Newton–Raphson method as implemented in GULP was used as

the energy minimizer. Hessian was updated every step by the scheme of Broyden–Fletcher–Goldfarb–Shanno (Shanno, 1970). When the gradient norm falls below a prescribed value of 0.002, the minimizer was switched to Rational Function Optimization (Banerjee et al., 1985) to accelerate the convergence and to generate a stable solution with positive eigenvalues of the Hessian matrix. Static structure optimization was used as well to determine the energetically favorable site for the cationic exchange $\text{Sr}^{2+} \leftrightarrow \text{Ca}^{2+}$ and the mechanical properties of the cementitious waste form as a function of strontium concentration $[\text{Sr}^{2+}]$. To perform this we distinguished between two Ca^{2+} sites in the bulk structure of C–S–H and 9 Å-tobermorite, i.e., the interlayer site and the polyhedral sheet site. To simulate the cation exchange in the interlayer sites, a Ca^{2+} cation in the interlayer space is chosen at random and replaced by Sr^{2+} , then the structure is optimized by allowing an all-atoms relaxations and simulation cell volume and shape relaxation. Upon full relaxation the elastic constants matrix is calculated, from which the bulk, shear and indentation moduli are calculated. This process is repeated until all the interlayer sites are exchanged. The same approach was applied to the polyhedral sheet sites but we stopped the exchange when a number of sites equal to the interlayer sites are exchanged. We did not fully exchange all the polyhedral sheets sites to provide a basis for the comparison between the two sites under consideration.

We performed six molecular dynamics (MD) simulations to study the structure stability of the strontium-substituted cementitious waste form and the coordination of the immobilized strontium. Two simulations were performed for the pure C–S–H and 9 Å-tobermorite, two simulations when all of the interlayer calcium sites are substituted with strontium, and finally two simulations when all the polyhedral sites are substituted. In all cases we performed 250 ps of equilibration in the isobaric–isothermal ensemble (NPT) at a pressure of 0 GPa and a temperature of 300 K. During these simulations, configurations with cell vectors close to the average equilibrium values were taken and used to start canonical ensemble (NVT) simulations. The production simulations in the NVT ensemble were 200 ps long. The code DL_POLY_2 (Smith et al., 2002; Smith, 2006) was used to perform the MD simulations. During the course of MD we treated the shells of the anions using the adiabatic approach described by Mitchell and Finchem (1993), whereby the shells were assigned a small mass of 0.2 atomic mass unit. A time step of 0.1 fs was used and Berendsen method was used to control both the pressure and temperature with a relaxation time of 0.5 ps for both the barostat and the thermostat. In all simulations, equations of motion were integrated using Verlet–Leapfrog algorithm.

2.3. Structural models

To represent the disordered C–S–H phase, we adopted the model developed by Pellenq et al. (2009). This model successfully accounts for many structural (radial distribution functions), mechanical (elastic constants) and chemical (Infra Red spectra) properties without being fitted to reproduce any of them (Pellenq et al., 2009). In addition, the properties of water confined in C–S–H studied by MD simulation utilizing this model (Youssef et al., 2011) were recently confirmed by quasielastic neutron scattering spectroscopy (Li et al., 2012). In Fig. 1, we show the atomic structure of this model. The model consists of two layers of calcium oxide and finite length silicate chains grafted on the calcium oxide layers. In addition, water molecules are trapped in the interlayer space and also trapped in small cavities within the calcium–silicate layers themselves. Moreover, interlayer calcium coexists with water in the interlayer space. 9 Å-tobermorite was modeled using the triclinic structure resolved by Merlino et al. (1999). It has layered structure with infinite silicate chains as is the case for the family

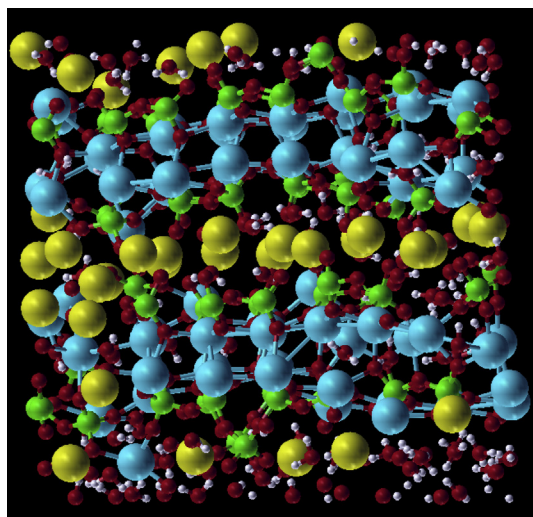


Fig. 1. Schematic of the recently developed atomistic model of C-S-H (Pellenq et al., 2009). It consists of two highly disordered layers of calcium-silicate and water molecules trapped in the interlayer space together with interlayer calcium ions. Few water molecules are trapped in small cavities in the calcium-silicate layers. White balls are hydrogen, red are oxygen, green are silicon, light blue are layer calcium and yellow are interlayer calcium. (For interpretation of the references to color in this figure legend, the reader is referred to the web version of this article.)

of tobermorite crystals. However, the calcium-silicate layers in the 9 Å-tobemrite are closer to each other (compared to other members of the family) and the mineral is completely dehydrated except from hydroxyl groups attached to silicon atoms. The very narrow channels between the calcium-silicate layers hosts only interlayer calcium. Fig. 2 is a depiction for 4 unit cells of this mineral. Table 1 gives a comparison between the disordered C-S-H and the 9 Å-tobemrite. The core-shell was successfully applied to study the disordered C-S-H (Pellenq et al., 2009), it remains to test its applicability to 9 Å-tobemrite. As a test, we compared the crystal structure properties of 9 Å-tobemrite predicted by static structure optimization and by isobaric-isothermal (NPT) molecular dynamics ($T = 300$ K, $P = 0$ GPa) with the experimentally determined structure (Merlino et al., 1999).

Table 2 summarizes the comparison and relative error. Although the c axis that is perpendicular to the calcium-silicate

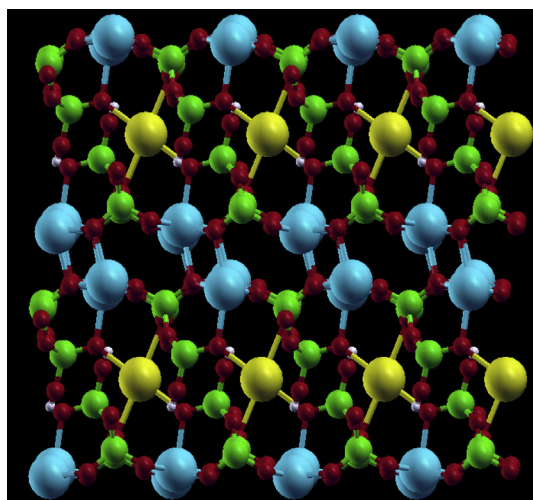


Fig. 2. Merlino structure for 9 Å-tobemrite (Merlino et al., 1999). Color code as in Fig. 1.

Table 1

Chemical composition and density of C-S-H and 9 Å-tobemrite.

	Disordered C-S-H	9 Å-tobemrite
Chemical formula	$(\text{CaO})_{1.65}-(\text{SiO}_2)-(\text{H}_2\text{O})_{1.73}$	$\text{Ca}_5\text{Si}_6\text{O}_{16}(\text{OH})_2$
Ca/Si	1.65	0.83
H/Si ^a	1.73	0.17
Cw/Ca _{poly} ^b	0.55	0.25
Density (g/cm ³) ^c	2.50	2.66

^a Strictly speaking this should be the water-to-silicon ratio. For 9 Å-tobemrite we count each two hydrogen atoms as if they belong to a dissociated water molecule.

^b This is the ratio between the interlayer calcium denoted by Cw and the layer (polyhedral sheets) calcium denoted by Ca_{poly}.

^c Calculated densities.

Table 2

Comparison of the structural properties of 9 Å-tobemrite derived from static structure optimization and NPT-MD with the experimentally determined structure (Merlino et al., 1999).

	Experimental	Structure optimization		NPT-MD	
		Value	Error %	Value	Error %
a axis (Å)	11.156	11.255	0.89	11.250	0.84
b axis (Å)	7.303	7.312	0.90	7.275	−0.38
c axis (Å)	9.566	10.096	5.54	10.553	10.32
α angle (°)	101.08	96.97	−4.06	98.62	−2.43
β angle (°)	92.83	88.12	−5.07	88.04	−5.16
γ angle (°)	89.98	89.30	−0.76	89.26	−0.80

layers is overestimated using the core-shell potential, we regard the agreement between the calculated and the experimental results good given that this force field was not fitted to the family of tobermorite and assumes high level of transferability for a large range of metal oxides.

3. Results and discussion

3.1. Energetically favorable exchange sites

Using static structure optimization, we calculated the potential energy of C-S-H and 9 Å tobermorite as a function of strontium substitution both in the interlayer sites and the polyhedral sites. The potential energy is used here as a metric to determine the favorable exchange site. Fig. 3 shows the results for both phases and for the two sites under consideration. In the case of C-S-H the substitution in the interlayer space is only slightly favorable at high substitution concentrations. At low concentration there is almost no distinction between them. This explains why it was difficult to determine by experiments which site is favorable, because in these experiments C-S-H was doped by a very low concentration of strontium (Tits et al., 2006; Wieland et al., 2008) and at such low concentrations, both sites seem to be equally favorable. On the other hand for 9 Å-tobemrite, it is clear that the substitution in the interlayer space is more favorable energetically compared to the polyhedral sheets substitution at all concentrations.

3.2. Structural stability and the binding environment

We used finite temperature molecular dynamics simulations to assess the stability of the structure of the two waste forms under consideration. Our specific metric in this context is the stability of the silicate chains grafted on the layers upon strontium substitution. The choice of this metric is based on an experimental study for the encapsulation of cesium (Cs^+) by C-S-H (Iwaida et al., 2002). In this study it was shown that Cs^+ breaks the silicate chains of C-S-H.

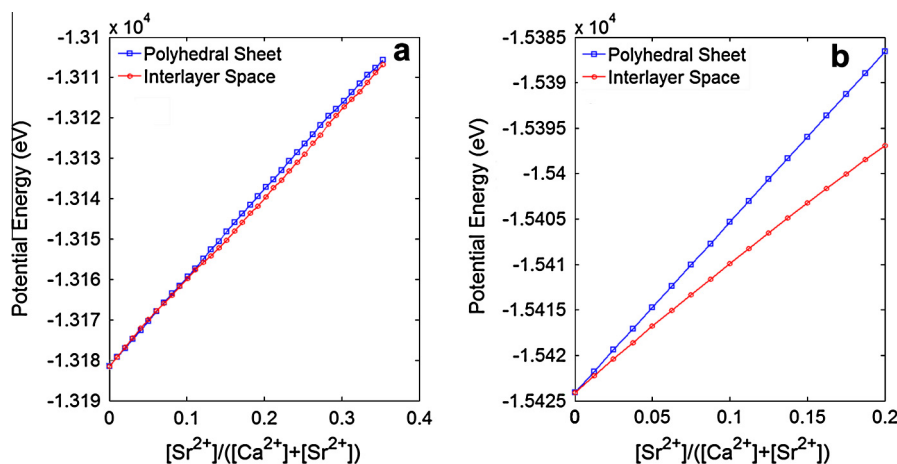


Fig. 3. The potential energy of (a) C-S-H and (b) 9 Å-tobermorite as a function of strontium substitution in the interlayer space sites and the polyhedral sheets sites, 1 eV = 96.4869 kJ/mol.

Table 3

A summary for bond lengths and the corresponding coordination numbers (N) around the bound strontium. The experimental results are taken from reference (Wieland et al., 2008).

	T (K)	Ca/Si	H/S	Sr-O (Å)	N	Sr-Si (Å)	N
C-S-H-interlayer	300	1.65	1.73	2.52	6.68	3.67	3.1
C-S-H/polyhedral	300	1.65	1.73	2.50	6.62	3.65	4.2
Tob/interlayer	300	0.83	0.17	2.49	4.24	3.64	6.2
Tob/polyhedral	300	0.83	0.17	2.49	7.08	3.64	5.5
C-S-H (exp)	77	0.7	–	2.60	6.3	–	–
C-S-H (exp)	77	1.1	–	2.61	7.6	4.33	2.0

The building block of the silicate chains is the silicate tetrahedron denoted by Q^n where $0 \leq n \leq 4$. Here n is the number of oxygen ions that bridge the central silicon ion to adjacent tetrahedra; thus Q^0 is an isolated tetrahedron, Q^1 occurs at the end of a chain, Q^2 resides in the middle of a chain, while Q^3 and Q^4 lead to complicated three dimensional structures (Taylor, 1997; Richardson,

2004). In our simulations we know the starting proportions of the different types of the tetrahedra in the pure C-S-H and 9 Å-tobermorite. For C-S-H these proportions are $Q^0 \sim 10\%$, $Q^1 \sim 67\%$ and $Q^2 \sim 23\%$, while for 9 Å-tobermorite, there are only Q^2 's as the silicate chains in this well-crystallized mineral are infinite in length. Full strontium substitution in the interlayer space or in the polyhedral sheet does not change these proportions of the silica tetrahedra in both waste forms within the simulation time considered here. This result shows that the structure of both waste forms is stable.

After demonstrating the stability of the structure of the waste forms we turn to discuss the coordination of the bound strontium cation Sr^{2+} . We characterize the coordination of the bound cation in terms of bond lengths and coordination numbers in the first nearest neighbors shell. In particular we calculated both the Sr-O bond length and the Sr-Si distance from the position of the first peak of the corresponding radial distributing functions. The coordination numbers for O and Si in the first shell around Sr were calculated by integrating these functions. These parameters can also be

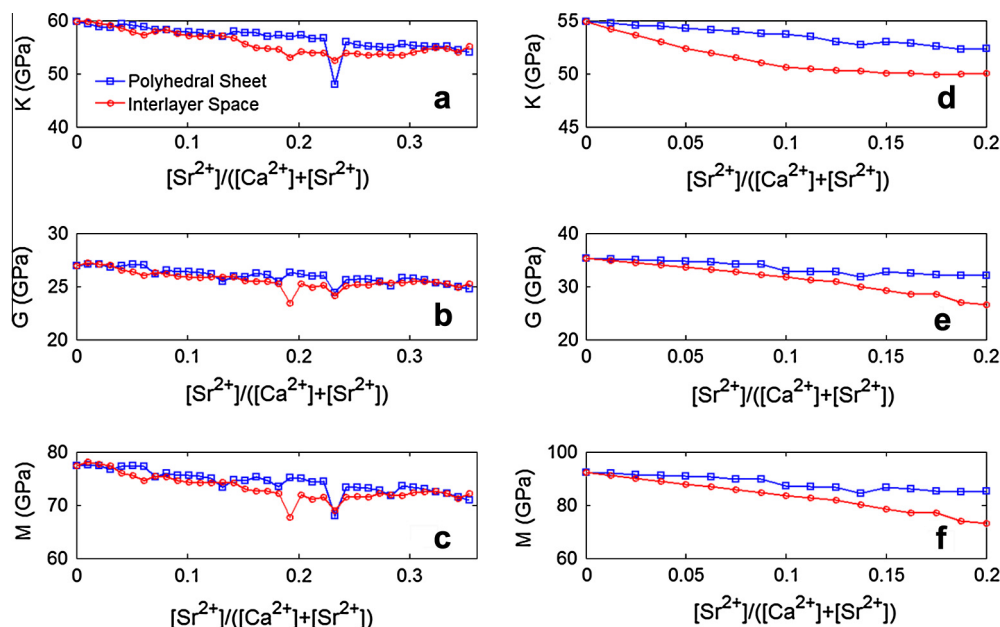


Fig. 4. The mechanical properties of the waste forms as a function of strontium substitution. (a), (b) and (c) are the bulk, shear and indentation moduli of C-S-H, respectively. (d), (e) and (f) are the bulk, shear and indentation moduli of 9 Å-tobermorite, respectively.

extracted from Extended X-ray Absorption Fine Structure (EXAFS) experiments (Wieland et al., 2008). In Table 3, we summarize the results obtained from our MD simulations accompanied with the results obtained from EXAFS experiments performed on Sr-doped C–S–H (Wieland et al., 2008).

The differences between the experiments and the simulations both in temperature and in chemistry do not allow straightforward comparison between them. However, we regard our results here as a demonstration that it is possible, in principle, to validate our computational models through EXAFS experiments by unifying the conditions under which simulations and experiments are conducted. Accomplishing this will render our computational models a powerful predictive tool.

3.3. The mechanical integrity of the waste form

Finally we assess the durability of the waste forms based on their mechanical integrity after the cationic exchange had taken place. For that purpose we calculated the bulk, shear and indentation moduli as a function of strontium substitution. These moduli contain information about the response of the waste form to various types of deformation. Shear (G) and bulk (K) moduli were calculated using Hill convention (Nye, 1985) while the indentation modulus (M) was determined by the relationship (Sneddon, 1965):

$$M = 4G \frac{3K + G}{3K + 4G}$$

Experimentally it is possible to measure a statistically significant indentation modulus for C–S–H by the grid indentation technique (Constantinides and Ulm, 2007), which makes our results regarding the mechanical integrity amenable to validation as well. Fig. 4 shows the obtained results for both C–S–H and 9 Å-tobermorite.

In general the mechanical properties degrade as the strontium concentration increases. The substitution in the interlayer space, which is energetically favorable, degrades the mechanical properties more than the substitution in the polyhedral sheet. This trend is more pronounced in 9 Å-tobermorite. It is expected that substitution in the interlayer space weakens the material more compared to the polyhedral sheet since these layered materials are generally weak in the interlayer direction and in addition to this the ionic radius of strontium is larger than that of calcium being next to it in the alkaline earth metal group. The consequence is that the substitution increases the thickness of the interlayer space which is the weakest plane direction. In spite of this, we believe that the overall degradation in these waste forms is not limiting and does not exclude cementitious materials as potential waste forms.

4. Conclusion

In this work, we addressed the issue of storing radionuclides in cement with the particular case of radioactive strontium-90 as a substituting element of pristine calcium species. We explored the potential use of two members of the calcium–silicate–hydrate family, disordered C–S–H (cement hydrate) and the mineral 9 Å-tobermorite, as waste forms to immobilize the radionuclide strontium-90 ($^{90}\text{Sr}^{2+}$) by means of atomistic simulations. Our results showed that the cationic exchange $\text{Sr}^{2+} \leftrightarrow \text{Ca}^{2+}$ is energetically favorable to take place in the interlayer space of both C–S–H and 9 Å-tobermorite with the trend more pronounced in the latter.

Furthermore this exchange does not affect the stability of the silicate chains in both waste forms within the time scale of our simulations. Finally we showed that the mechanical properties degrade as strontium concentration increases in the waste form,

however, we believe that this degradation is not severe and hence does not limit the use of cement as a waste form for strontium. Several studies (Ma et al., 1996; Tsuji and Komarneni, 1989) showed that aluminum-substituted C–S–H and tobermorite have a larger capacity to immobilize metal cations compared to the pure phases. In future studies, we can consider aluminum-substituted phases as initial models (Abdolhosseini Qomi et al., 2012). Moreover, it was shown recently by Tits et al. (2006) and Mandaliev et al. (2010) that neodymium substitution in hydrated tobermorite is accompanied by a partial release of the water molecules in the interlayer space. This reflects the fact that the equilibrium hydration level can change by substituting new elements in the structure of the hydrated C–S–H phases. This can also be addressed in the future by performing grand canonical Monte-Carlo simulations at each cationic exchange step to determine the equilibrium hydration level.

Acknowledgments

This work was sponsored (i) by the MIT Concrete Sustainability Hub, supported by the Portland Cement Association (PCA) and the Ready Mix Concrete (RMC) Research & Education Foundation, and (ii) by the Center for Advanced Nuclear Energy Systems (CANES) at MIT.

Appendix A. Supplementary material

Supplementary data associated with this article can be found, in the online version, at <http://dx.doi.org/10.1016/j.pce.2013.11.007>.

References

- Abdolhosseini Qomi, M.J., Ulm, F.-J., Pellenq, R.J.-M., 2012. Evidence on the dual nature of aluminum in the calcium–silicate–hydrates based on atomistic simulations. *J. Am. Ceram. Soc.* 95, 1128–1137.
- Allen, M., Tildesley, S., 1987. *Computer Simulation of Liquids*. Oxford Press, New York.
- Allen, A., Thomas, J., Jennings, H., 2007. Composition and density of nanoscale calcium–silicate–hydrate in cement. *Nat. Mater.* 6, 311–316.
- Ansolabehere, S., Deutch, J., Driscoll, M., Gray, P., Holdren, J., Joskow, P., Lester, R., Moniz, E., Todreas, N., Beckjord, E., Hottle, N., Jones, C., Parent, E., 2003. The Future of Nuclear Power, an interdisciplinary MIT study. <<http://web.mit.edu/nuclearpower/>>.
- Banerjee, A., Adams, N., Simons, J., Shepard, R., 1985. Search for stationary-points on surface. *J. Phys. Chem.* 89, 52–57.
- Constantinides, G., Ulm, F.-J., 2007. The nanogranular nature of C–S–H. *J. Mech. Phys. Solids* 55, 64–90.
- de Leeuw, N.H., Parker, S.C., 1998. Molecular-dynamics simulation of MgO surfaces in liquid water using a shell-model potential for water. *Phys. Rev. B* 58, 13901–13908.
- Dick, A., Overhauser, B., 1958. Theory of the dielectric constant of alkali halide crystals. *Phys. Rev.* 112, 90–103.
- Evans, N.D.M., 2008. Binding mechanisms of radionuclides to cement. *Cem. Concr. Res.* 38, 543–553.
- Gale, J., 1996. Empirical potential derivation for ionic materials. *Philos. Mag.* B 73, 3–11.
- Gale, J., Rohl, A., 2003. The General Utility Lattice Program (GULP). *Mol. Simul.* 29, 291–341.
- Higgins, F.M., de Leeuw, N.H., Parker, S.C., 2002. Modeling the effect of water on cation exchange in zeolite A. *J. Mater. Chem.* 12, 124–131.
- Iwaida, T., Nagasaki, S., Tanaka, S., Yaita, T., Tachimori, S., 2002. Structure alteration of C–S–H (calcium silicate hydrated phases) caused by sorption of caesium. *Radiochim. Acta* 90, 677–681.
- Kalinichev, A.G., Wang, J.W., Kirkpatrick, R.J., 2007. Molecular dynamics modeling of the structure, dynamics and energetics of mineral–water interfaces: application to cement materials. *Cem. Concr. Res.* 37, 337–347.
- Kerisit, S., Parker, S.C., 2004. Free energy of adsorption of water and metal ions on the {1014} calcite surface. *J. Am. Chem. Soc.* 126, 10152–10161.
- Kerisit, S., Cooke, D., Spagnoli, D., Parker, S.C., 2005. Molecular dynamics simulations of the interaction between the surfaces of polar solids and aqueous solutions. *J. Mater. Chem.* 15, 1454–1462.
- Kerisit, S., Ilton, E., Parker, S.C., 2006. Molecular dynamics simulations of electrolyte solutions at the (100) goethite surface. *J. Phys. Chem. B* 110, 20491–20501.
- Komarneni, S., Roy, D.M., 1983. Tobermorites: a new family of cation exchangers. *Science* 221, 647–648.

- Komarneni, S., Roy, R., Roy, D.M., 1986. Pseudomorphism in xonotlite and tobermorite with Co^{2+} and Ni^{2+} exchange for Ca^{2+} at 25 °C. *Cem. Concr. Res.* 16, 47–58.
- Komarneni, S., Brevet, E., Roy, D.M., Roy, R., 1988. Reaction of some calcium silicates with metal cations. *Cem. Concr. Res.* 18, 204–220.
- Kundu, T., Rao, H., Parker, S.C., 2005. Competitive adsorption on wollastonite: an atomistic simulation approach. *J. Phys. Chem. B* 109, 11286–11295.
- Lewis, G.V., Catlow, C.R.A., 1985. Potential models for ionic oxides. *J. Phys. C: Solid State Phys.* 18, 1149–1161.
- Li, H., Fratini, E., Chiang, W.-S., Baglioni, P., Mamontov, E., Chen, S.-H., 2012. Dynamic behavior of hydration water in calcium–silicate–hydrate gel: a quasielastic neutron scattering spectroscopy investigation. *Phys. Rev. E* 86, 061505.
- Ma, W., Brown, P.W., Komarneni, S., 1996. Sequestration of cesium and strontium by tobermorite synthesized from fly ashes. *J. Am. Ceram. Soc.* 79, 1707–1710.
- Mandaliev, P., Wieland, E., Dähn, R., Tits, J., Churakov, S.V., Zaharko, O., 2010a. Mechanisms of Nd(III) uptake by 11 Å tobermorite and xonotlite. *Appl. Geochem.* 25, 763–777.
- Mandaliev, P., Dähn, R., Tits, J., Wehrli, B., Wieland, E., 2010b. EXAFS study of Nd(III) uptake by amorphous calcium silicate hydrates (C–S–H). *J. Colloid. Interface Sci.* 342, 1–7.
- Merlino, S., Bonaccorsi, E., Armbruster, T., 1999. Tobermorites: their real structure and order–disorder (OD) character. *Am. Miner.* 84, 1613–1621.
- Mitchell, P., Fincham, D., 1993. Shell model simulation by adiabatic dynamics. *J. Phys.: Condens. Matter* 5, 1031–1038.
- Nye, J.F., 1985. *Physical Properties of Crystals*. Oxford University Press, New York.
- Pelleng, R.J.-M., Kushima, A., Shahsavari, R., Van Vliet, K.V., Buehler, M., Yip, S., Ulm, F.-J., 2009. A realistic molecular model of cement hydrates. *Proc. Natl. Acad. Sci. USA* 106, 16102–16107.
- Richardson, I.G., 2004. Tobermorite/jennite- and tobermorite/calcium hydroxide-based models for the structure of C–S–H: applicability to hardened pastes of tricalcium silicate, beta-dicalcium silicate, Portland cement, and blends of Portland cement with blast-furnace slag, metakaolin, or silica fume. *Cem. Concr. Res.* 34, 1733–1777.
- Shanno, D.F., 1970. Conditioning of the quasi-Newton methods for function minimization. *Math. Comp.* 24, 647–658.
- Smith, W., 2006. DL-POLY: to molecular simulation II. *Mol. Simul.* 32, 933.
- Smith, W., Yong, C., Rodger, P., 2002. DL-POLY: application to molecular simulation. *Mol. Simul.* 28, 385–471.
- Sneddon, I.N., 1965. The relation between load and penetration in the axisymmetric boussinesq problem for a punch of arbitrary profile. *Int. J. Eng. Sci.* 3, 47–57.
- Spagnoli, D., Cooke, D., Kerisit, S., Parker, S.C., 2006. Molecular dynamics simulations of the interaction between the surfaces of polar solids and aqueous solutions. *J. Mater. Chem.* 16, 1997–2006.
- Taylor, H.F.W., 1997. *Cement Chemistry*. Thomas Telford, London.
- Tits, J., Wieland, E., Müller, C.J., Landesman, C., Bradbury, M.H., 2006. Strontium binding by calcium silicate hydrates. *J. Colloid. Interface Sci.* 300, 78–87.
- Tsuji, M., Komarneni, S., 1989. Alkali metal ion exchange selectivity of Al-substituted tobermorite. *J. Mater. Res.* 4, 698–703.
- Wieland, E., Johnson, C.A., Lothenbach, B., Winnefeld, F., 2006. Mechanisms and modeling of waste/cement interactions – Survey of topics presented at the Meiringen Workshop. In: *Mater. Res. Soc. Symp. Proc.* 932, pp. 663–671.
- Wieland, E., Tits, J., Kunz, D., Dähn, R., 2008. Strontium uptake by cementitious materials. *Environ. Sci. Technol.* 42, 403–409.
- Youssef, M., Pelleng, R.J.-M., Yildiz, B., 2011. Glassy nature of water in an ultraconfining disordered material: the case of Calcium–Silicate–Hydrate. *J. Am. Chem. Soc.* 133, 2499–2510.